J Geod (2012) 86:209–219
DOI 10.1007/s00190-011-0511-x

ORIGINAL ARTICLE

GPS snow depth meter with geometry-free linear combinations of carrier phases

Masaru Ozeki · Kosuke Heki

Received: 7 March 2011 / Accepted: 26 August 2011 / Published online: 14 September 2011

Abstract Multipath in global positioning system (GPS) is the interference of the microwave signals directly from satellites and those reflected before reaching the antenna, typically by the ground. Because reflected signals cause positioning errors, GPS antennas are designed to reduce such interference. Recent studies show that multipath could be utilized to infer the properties of the ground around the antenna. Here, we report one such application, i.e. a fixed GPS station used as a snow depth meter. Because the satellite moves in the sky, the excess path length of reflected waves changes at rates dependent on the antenna height. This causes quasi-periodic variations of the amplitude and phase of the received signals. Accumulation of snow reduces effective antenna heights, and we can see it by analyzing multipath signatures. Signal-to-noise ratios (SNR) are often used to analyze multipath, but they are not always available in raw GPS data files. Here, we demonstrate that the geometry-free linear combination (L4), normally used to study the ionosphere, can also be used to analyze multipath signatures. We obtained snow depth time series at a GPS station in Hokkaido, Japan, from January to April in 2009 using L4 and SNR. Then, we compared their precisions. We also discuss mechanisms responsible for the possible underestimation of the snow depth by GPS. Finally, we investigate the possibility of inferring physical conditions of the snow surface using amplitudes of multipath signatures.

Keywords GPS · Snow depth · Multipath · Linear combination · SNR

1 Introduction

The global positioning system (GPS) was developed originally as a military navigational aid. It has been used also by civilian users for various purposes, including automotive navigation, operational control of ships and aircraft, orbit determination of satellites in low orbits, and measurement of tectonic plate movements (Hofman-Wellenhof et al. 2001). In addition to positioning, applications of GPS for remote sensing of tropospheric water vapor (Shoji et al. 2009) and ionospheric electrons (Mannucci et al. 1998) have been explored and come into practical use. GPS like networks now constitute a part of the global infrastructure for variety of disciplines in geophysics. Over the last few years, several new GPS applications using multipath have been explored.

Multipath is the interference between direct microwave signals from the satellites and those reflected before reaching the antenna, typically by the ground. The reflected signals cause, e.g. positioning errors repeating with a period close to a sidereal day (∼4 min shorter than a solar day) because the orbital period of the GPS satellites is half a sidereal day. Although GPS antennas are designed to attenuate waves (signals) from negative elevations in order to minimize such errors, a certain amount of reflected waves leak into receivers under low elevation conditions. A typical pattern of GPS antennas is available in Bilich et al. (2008).

Larson et al. (2008a,b) first proposed to make positive use of multipath without modifying existing geodetic GPS stations. They demonstrated that the phase of the multipath contains information on the near-surface soil moisture around the antenna. Later, Larson et al. (2009) and Small et al. (2010) expanded the application of the multipath analyses for changes in snow depths and vegetation around the antenna.

M. Ozeki · K. Heki (✉)
Department of Natural History Sciences, Hokkaido University,
N8 W10 Kita-ku, Sapporo, Hokkaido, Japan
e-mail: heki@mail.sci.hokudai.ac.jp

Although amplitudes and phases of the L-band carrier waves include multipath signatures, it is difficult to isolate them because changes coming from various factors have to be removed. Larson et al. (2008a) proposed to use the signal-to-noise ratio (SNR) to study multipath. SNR indicates the strength of received microwave signal. It is geometry-free, i.e. it does not depend on geometric parameters such as the coordinates of antennas and satellites, and is handy to extract multipath signatures. However, SNR is not always included in the raw GPS data files distributed worldwide because it was thought to be of little use for most users of GPS.

Another observable is the geometry-free linear combination of the phases of the two L-band carriers L1 (1.57542 GHz) and L2 (1.22760 GHz). It is always available and can be used to study multipath. In the ionosphere, solar radiation ionizes a part of the atmosphere, and electrons there cause a propagation delay which is to first order inversely proportional to the square of the frequency (Kedar et al. 2003). For positioning purposes, we remove ionospheric delays by making an ionosphere-free linear combination of L1 and L2. The ionospheric linear combination (L4) is the simple difference between L1 and L2

$$\mathrm{L4} \equiv \mathrm{L1} - \mathrm{L2}. \tag{1}$$

Because the geometric information has been cancelled by taking the difference, L4 is also geometry-free (L4 includes ionospheric delays, phase biases, multipath terms, and noise). Here L1 and L2 are multiplied by wavelengths, and have units of length. L4 is convenient to extract information on the number of electrons integrated along the line of sight, called Total Electron Content (TEC). Therefore, L4 is widely used to study various kinds of ionospheric disturbances, including coseismic ionospheric disturbances (Heki and Ping 2005) and formation of ionospheric holes (Ozeki and Heki 2010).

In this article, we compare the snow depths obtained using SNR and L4 data. If L4 could be used for multipath analyses, it would expand the target of these multipath approaches to most of the geodetic GPS stations worldwide installed on the ground. We could also go back in time to the 1990s and study climatological changes of snow depths over the last two decades. Preexisting networks of conventional snow depth meters are not sufficient in many places in the world. In addition, it is difficult to measure snow depths by remote sensing. When considering these points, even the inference of snow depths with 10–20% uncertainties would significantly contribute to hydrological and climatological studies (Larson et al. 2009). Apart from the depth, we will also discuss a possibility to infer physical status, e.g. water content and density, of the snow by analyzing the multipath.

2 Principles of GPS snow depth meter

2.1 GPS antenna height (snow depth) and multipath

Interference of the wave reflected at the ground causes a phase shift to the total (i.e. reflected plus direct) received microwave signal. Because the phase shift $\delta\varphi$ is a function of satellite elevation ε (Eloségui et al. 1995),

$$\delta\varphi(\varepsilon, \alpha, H, \lambda) = \tan^{-1} \frac{\alpha \sin\left(4\pi \frac{H}{\lambda} \sin\varepsilon\right)}{1 + \alpha \cos\left(4\pi \frac{H}{\lambda} \sin\varepsilon\right)}, \tag{2}$$

it changes as the satellite moves in the sky. H is the GPS antenna height (Fig. 1a), and λ is the wavelength. The ratio of the amplitude of the reflected wave relative to the direct wave is indicated by α. It depends both on the reflectivity of the ground (snow) surface and the antenna gain pattern. The accumulation of snow lets the apparent height H decrease to H' (Fig. 1b). So we try to estimate H to infer snow depths.

Because the GPS satellite moves in the sky, changing elevation angle causes the excess path length to vary in time. The alternation of constructive and destructive interference causes quasi-periodic variations of the phases and amplitudes of the received L1 and L2 (and hence their difference, L4) signals. Figure 2a shows such "multipath signatures" at the Shinshinotsu GPS site (see Sect. 3) synthesized using Eq. (2) and the satellite 19 orbit. The multipath signature amplitudes depend on α while their periods depend on the antenna height. An antenna with smaller height shows a longer period because its excess path length changes more slowly. The L4 signature is the mixture of fluctuations of the L1 and L2 phases, and we see their beat signals (Fig. 2a).

Larson et al. (2008a,b) estimated the phase shift of the multipath signature to infer the apparent change in the position of the ground reflector, which normally lies ∼5 cm below the surface and gets shallower as rain brings moisture to the near surface soil. In this study, we performed spectral analysis for the multipath signatures rather than estimating the phase shift. This is partly because the larger antenna heights (∼5 m) in our case resulted in higher frequency multipath signatures than Larson et al. (2008a,b), who used a lower (∼2 m) antenna. We could easily separate two spectral peaks coming from L1 and L2 with this approach (Fig. 2b).

As can be seen in Fig. 2a, the periods of the multipath signatures are not constant. They change little for elevations lower than 30° (in Fig. 2a, frequencies of the multipath signatures are ∼4.5 and ∼4.3 mHz at the elevations of ∼5° and ∼30°, respectively), but lengthen as the satellites further ascend. As suggested by Eq. (2), the period could be kept almost constant by replacing time t with $\sin\varepsilon$. In that case, however, we need a more sophisticated tool

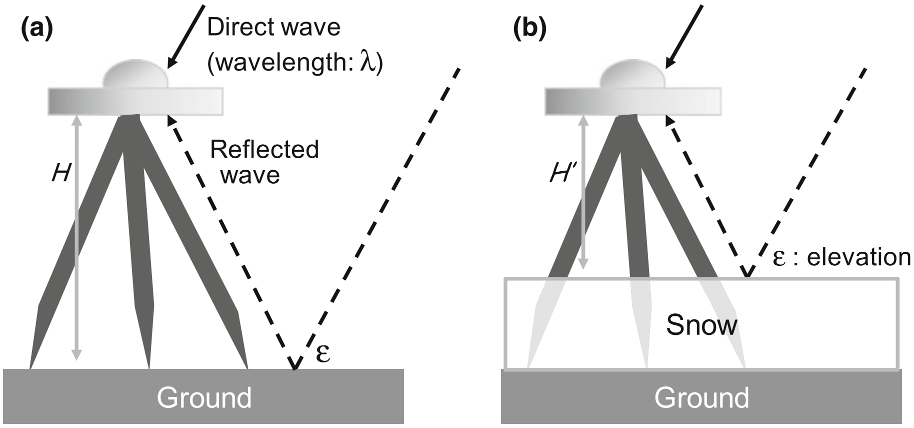

Fig. 1 **a** Multipath is the interference between the direct and reflected waves. The excess path length of the reflected wave changes as the satellite moves in the sky at a rate depending on the antenna height H, which decreases to H' as snow accumulates on the ground (**b**)

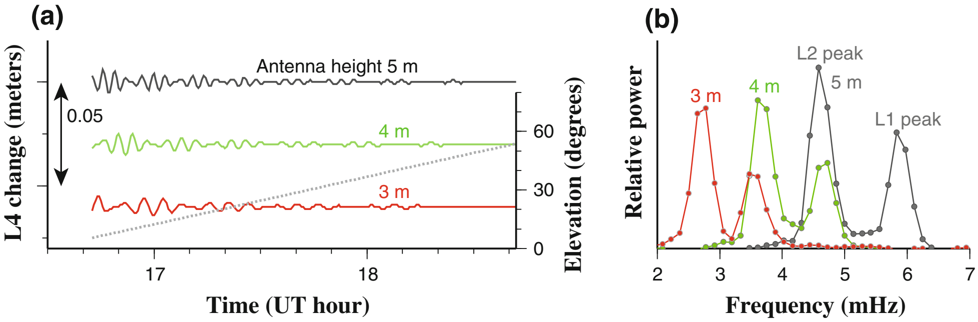

Fig. 2 **a** Temporal changes of the L4 phase (m) calculated for the first 2 h after the rise of the satellite 19 on March 1, 2009, at the Shinshinotsu (020877) GPS station, using Eq. (2) assuming three different heights of antenna (3, 4 and 5 m, which means snow depths of 2, 1, and 0 m because the original antenna height is 5 m). We calculated α assuming 0.15 for the microwave reflectivity at the ground and the antenna pattern given in Bilich et al. (2008). The *gray dotted line* shows the change in the satellite elevation. **b** Spectrogram of the three L4 phase time series in **a** are composed of two distinct peaks originating from phase changes of L1 and L2. We use the L2 peak (the one with the lower frequency) to estimate snow depths

for spectral analysis capable of handling irregular sampling intervals, such as the Lomb–Scargle periodogram (Larson et al. 2009). Practically, the gain pattern of the antenna attenuates the reflected signals for high elevations, and so the spectrogram in Fig. 2b reflects multipath signatures, while the satellite is relatively low. Thus, spectral peaks remain sharp enough to constrain antenna heights with some precision (Fig. 2b). We show later that the spectrograms based on the multipath signatures of the real GPS data show similar features of spectral peaks to Fig. 2b.

2.2 Conversion from peak frequency to snow depth

We performed spectral analysis of the observed L4 phase time series using the Blackman–Tukey method (e.g. Hino 1984) assuming constant periods of the multipath signatures (see Sect. 2.2 for the actual range of period changes). Because L4 is the linear combination of L1 and L2, its spectrogram has two peaks (Fig. 2b). In this study, we use the L2 peaks because they usually showed clearer spectral peaks than L1. We also analyzed the L2 SNR time series to obtain their spectral peaks. To determine the peak position, we took the frequency with the highest power (from the frequency range corresponding to snow depths between zero and one meter) and the two frequencies at either side. Then, we fit a quadratic function to the three points, and determined the precise position of the peak.

The approximate height of the antenna of the GEONET GPS stations is 5 m, and the L2 multipath signature under the snow-free condition is ~4.5 mHz (period ~3.7 min) for the case in Fig. 2. This frequency peak becomes lower as the snow pack develops: it decreases by ~0.75 mHz for the snow depth of 1 m (i.e. apparent antenna height 4 m) (Fig. 2b). By performing the spectral analyses for the synthesized data, we made "calibration curves" to convert the multipath signature frequency to the antenna height (Fig. 3). Actually, the curves are linear for realistic snow depth ranges. The decrease in antenna height means an increase in snow depth. The biases (antenna height under the snow-free condition) may differ somewhat from 5 m (e.g. dry soil at Marshall, Colorado, USA, is known to have effective reflector depth of ~5 cm, see Larson et al. (2008b). Therefore, such biases were tuned a posteriori by adjusting the estimated snow depth in the snow-free period in April to zero.

The calibration curve has to be tuned separately for different satellites, as well as for different GPS sites. For example,

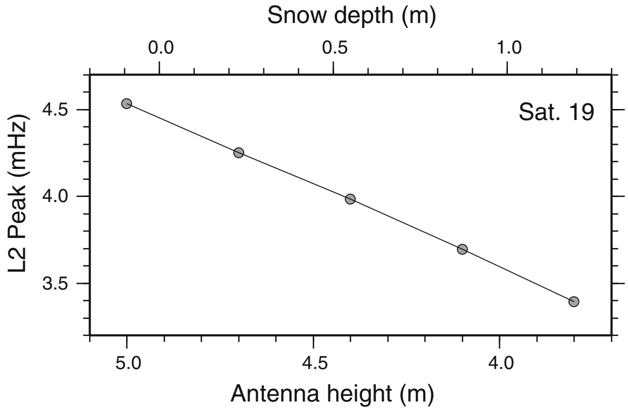

Fig. 3 Calibration curve to relate the L2 peak frequency to the snow depth inferred from synthesized multipath signatures as shown in Fig. 2a. The calibration equation is expressed as (Snow depth) (m) = {4.4 − (Frequency peak) (mHz)}/0.93. This *curve* is valid only for the ascending satellite 19 received at the Shinshinotsu GPS station

the gradients of the curves depend on the changing rates of satellite elevation and hence on satellite orbits (this dependence disappears by replacing the time with $\sin\varepsilon$). The biases may also depend on satellites because the ground where the snow reflects microwave signal may not be flat. For the five satellites used in this study, the gradient of the calibration curve varied between 0.86 and 0.93 mHz/m. The same calibration curve is used for L4 and SNR. The difference of reflectivity at the snow surface depends on the physical condition of the snow–air boundary. This difference changes α in Eq. (2), but does not significantly influence the periods of the multipath signatures.

3 Observation results

3.1 Observing site and period

GPS Earth Observation Network (GEONET) is operated by the Geospatial Information Authority (GSI) of Japan (anonymous ftp available at ftp://terras.gsi.go.jp). In this study, we used data at one of the GEONET GPS stations 020877 in Shinshinotsu, ∼30 km northeast of Sapporo, Hokkaido, from January 1 to April 16, 2009. The receiver is a Trimble 5700, and the antenna TRM29659.00 is covered with a hemispherical radome. During this period, there was an open ground to the south of the antenna, and this enabled us to analyze multipath signatures of several satellites in the southern sky. The aerial photograph is given in Fig. 4a. This picture was taken after the construction of a building started to the south of the GPS antenna in spring 2009 (see Sect. 5). The area is in the middle of a flat alluvial plain. There is an AMeDAS (Automatic Meteorological Data Acquisition System) ultrasonic snow depth sensor about 500 m west of the GPS antenna (Fig. 4a, inset). This is operated by the Japan Meteorological Agency (JMA), and the data are available online from http://www.jma.go.jp/en/amedas/. So this is a good site to compare snow depths from GPS (L4 and SNR) with those measured in a conventional way.

We analyzed data over 2-h periods of the descending satellites 18, 21, and 24 before the satellites set and the ascending satellite 19 and 29 after the satellites rose. Data are available for elevation angles higher than ∼5°. We plot the trajectory of the ground reflection points in Fig. 4b (paths marked with thick curves). The whole trajectory scales with the antenna height (5 m in the figure), i.e., trajectories shrink toward the antenna as snow accumulates. The observing time window was synchronized with the sidereal day (i.e. shifted forward by ∼4 min every day) to keep the same satellite positions in the sky.

We show the behavior of the L4 (Fig. 5a) and SNR (Fig. 5b) for satellite 19 during March 2009 at this GPS station for a time window of ∼1 h after the receiver started to record the satellite signal. The L4 data include changes coming from ionosphere, i.e. diurnal variations of vertical TEC and variations in slant TEC due to the satellite elevation changes. Hence, they were high-pass filtered by polynomial fitting to remove these components (here we used degree 10 over the 2-h window to remove components with periods longer than ∼0.5 h). High frequency variations with periods ∼4 min (the approximate period for snow-free condition) or less are the multipath signatures. The L4 time series still show low frequency variations possibly coming from insufficient removal of ionospheric changes. On the other hand, clearer multipath signatures are seen in the SNR data (Fig. 5b). They are free from such long-period variations of ionospheric origins and we just removed quadratic function components coming from elevation changes. Figure 6 shows spectrograms of L4 multipath signatures of five selected days.

3.2 Snow depth estimated with L4 and SNR

Figure 7 shows the snow depths estimated by analyzing L4 data from five different satellites, 18, 19, 21, 24, 29 in the southern sky (Fig. 4b). The overall trends of the snow depths estimated by individual satellites (Fig. 7a) show similar behaviors to AMeDAS, but individual satellite data are scattered by a few tens of centimeters. The data seem noisier in January, and less so in March. Wet and dense spring snow may reflect more microwave signal resulting in clearer spectral peaks of multipath signatures. Therefore, such a difference in signal-to-noise ratios may reflect the difference in the snow surface. This point will be discussed in Sect. 4.

Outliers would have come from wrong identification of spectral peaks because the program automatically selects the frequency with the largest power in a given spectral range. For a better identification of spectral peaks, we stacked the

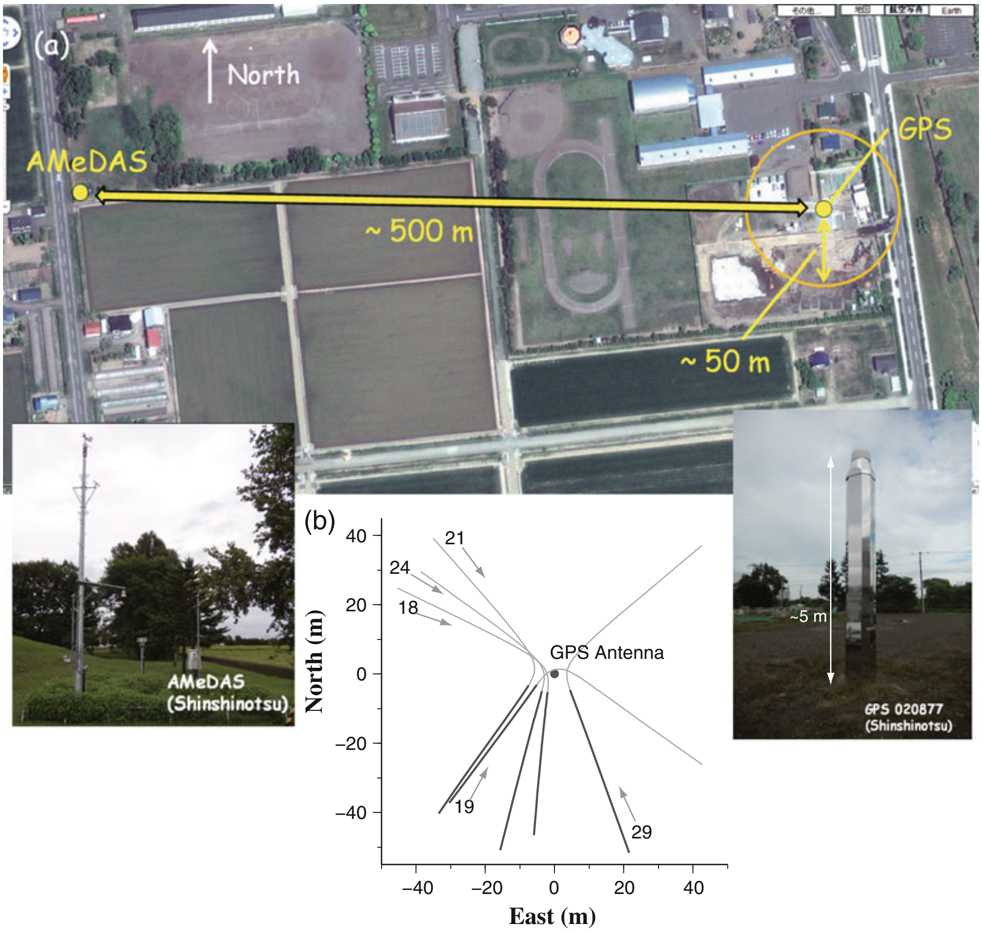

Fig. 4 **a** The Shinshinotsu site with a GEONET GPS antenna (*right inset*), and an AMeDAS snow depth sensor (*left inset*) ∼500 m to the west. Ground reflection points responsible for multipath are within ∼50 m from the antenna (*yellow circle*). Aerial photograph is from the Google Map. In **b**, we show the reflection point trajectories of five GPS satellites analyzed in this study (actual footprints have diameters of a few meters coming from the first Fresnel zone). A *black dot* indicates the GPS antenna. *Thick parts of the curves* are used for the analysis of snow depths

spectrograms of three consecutive days to find the spectral peak on the middle day. By moving the 3-day window day by day, we smoothed the time series (Fig. 7b). There unrealistic snow depths have disappeared. Next, we calculated the daily averages (error bars show their one standard deviations) of the snow depths from the five GPS satellites (Fig. 7c). The average of the standard deviations of all the days is ∼6 cm, which indicates the precision of the L4 GPS snow depth meter. We compared the GPS and AMeDAS results, and found that the GPS results tend to be smaller than the AMeDAS data by ∼10 cm. We will discuss this in Sect. 4.

Data processing similar to L4 has been done for the same satellites using SNR data of the L2 carrier. We used the same equation as L4 to convert the spectral peak to the snow depth. It is obvious in Fig. 5 that multipath signatures are more clearly seen in SNR data than in L4 data. Consequently, snow depths recovered using the SNR data (Fig. 8) are less noisy than L4 (Fig. 7). The precision of the SNR data (standard deviation of all the snow depths from the five satellites) was ∼4 cm, about two-thirds of L4. These results suggest that it is better to use SNR if both quantities are available. We currently use SNR of L2P, and switching it to the more accurate L2C might further improve the results (K. Larson, personal communication). The SNR results show a negative bias from the AMeDAS data similar to L4.

4 Discussion

4.1 Negative bias of GPS results

The snow depths estimated by GPS multipath signatures in L4 (Fig. 7) and SNR (Fig. 8) are about ∼ 0.1 m lower than those by the AMeDAS conventional snow depth meter (located ∼500 m to the west (Fig. 4a). One possibility for this difference is that this reflects the real difference in snow depth between the two points. It is difficult to verify this because there were no in situ snow depth measurements around the

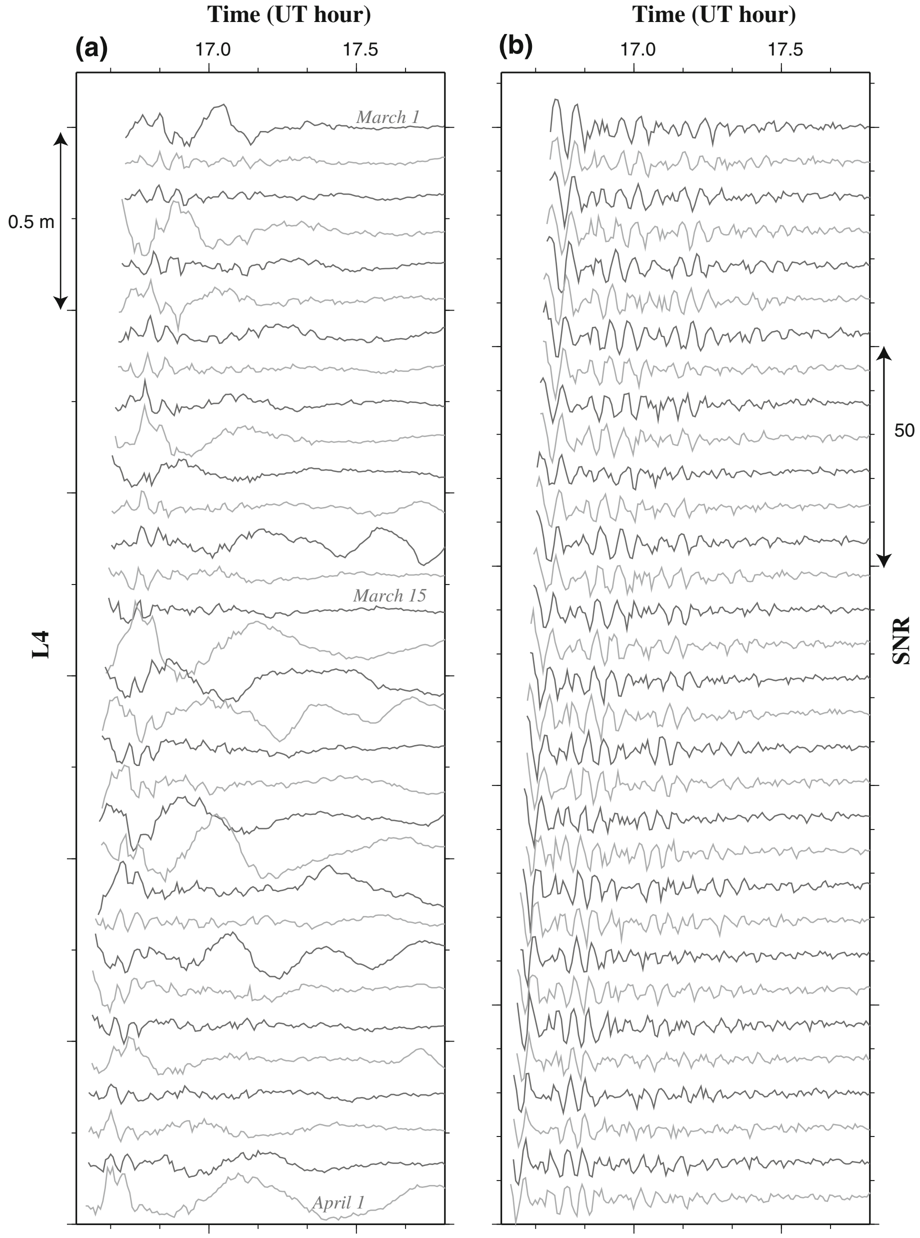

Fig. 5 The time series of L4 (**a**) and SNR (**b**) from 1 March to 1 April, 2009, of satellite 19 at the Shinshinotsu GPS station. The *label* of the *horizontal axis* at the *top* is valid only for the uppermost time series because the observing window is shifted ∼4 min earlier per day to keep the same satellite positions in the sky

reflection point trajectories shown in Fig. 4b. Although there are no hills or mountains within a few tens of kilometers, there are some trees and low buildings within 100 m of the antenna that might have caused minor snow depth irregularities. Therefore, a real snow depth difference of 10 cm cannot be ruled out.

Here, we discuss the possibility that the underestimation reflects the penetration of the microwave signal into the snow. Although the waves are partly reflected at the snow surface as a specular reflector, some part penetrates into the snow and are scattered. The scattered microwave signal partly reaches the antenna with slightly longer excess paths, and causes the underestimation of snow depths (or overestimation of antenna heights). Microwave signals also penetrate into soil, and Larson et al. (2008b) showed effective reflector depths of ∼5 cm for dry soils in Marshall, Colorado (it gets less for wet soils). We tuned the calibration curves (e.g. Fig. 3 for satellite 19) empirically so that snow depths are zero in April. Hence, the underestimation of GPS snow depth meter in Figs. 7 and 8 suggests that the effective reflector depth of snow is greater than soil by ∼10 cm.

Penetration depth of microwave depends on the frequency and the complex permittivity of the snow. Zavorotny et al. (2010) showed the near surface complex permittivity of dry soil was ∼4.0 (real part) and ∼0.5 (imaginary part). This permittivity causes a L2 penetration depth of ∼0.16 m. According to Iizaka (1998), fresh snow in mid-winter (density 100 kg m^{-3}, and 5% liquid water by weight) would

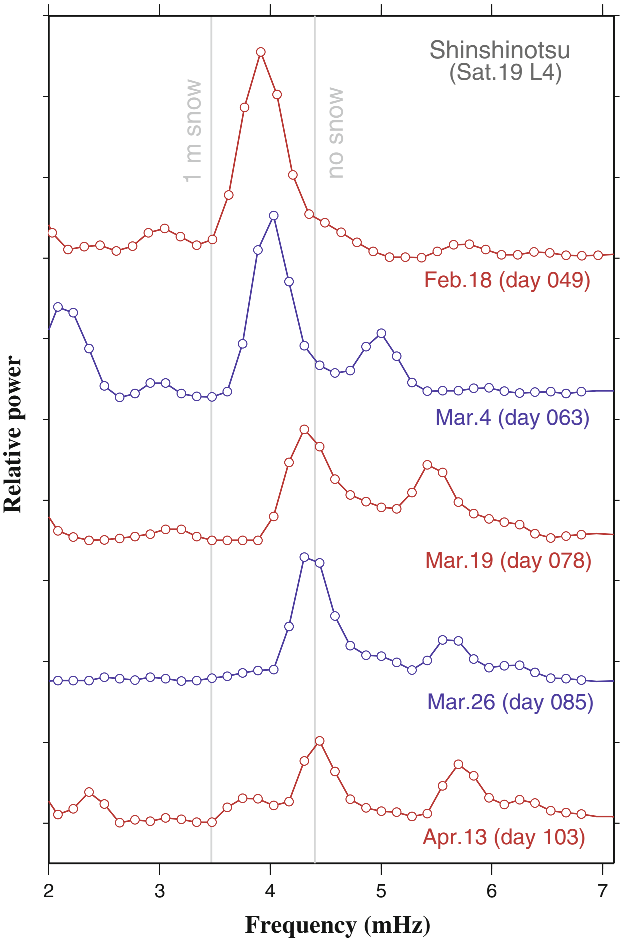

Fig. 6 The spectrograms of the L4 multipath signatures of the rising satellite 19 observed at the Shinshinotsu GPS station on five selected days from February to April, 2009. Positions of the peaks contain the information on the snow depths. The *two gray vertical lines* correspond to no snow and 1 m snow

have the real and imaginary parts of its complex permittivity of ~2.0 and ~0.10, respectively. This allows the L2 penetration of ~0.55 m (or more for drier snows). Spring wet snow (density 500 kg m^{-3}, and 20% liquid water by weight) would have the permittivity of ~6.0 (real part) and ~0.35 (imaginary part), and the L2 penetration depth of ~0.27 m. Microwave signals thus penetrate significantly deeper into snow than soil whatever the snow condition. Assuming that a larger effective reflector depth is caused by the deeper L-band penetration, difference of the effective reflector depth of ~10 cm between the snow and the soil might be possible.

Both the penetration depth and surface reflectivity depend on the density and water content of surface snow. Theoretically, microwave signals penetrate deeper into dry and porous snows, and such snows reflect microwave signals more weakly than wet and dense snows at their surfaces. In Fig. 9, we examine if the snow depth biases (representing microwave signal penetration) are negatively correlated with the power of the frequency peaks (representing surface reflectivity). We do not see significant correlation between them, suggesting the depth of the effective reflector remains similar (~10 cm deeper than soil) irrespective of the snow condition. Probably, we would have needed more precision to see such correlation.

4.2 Peak strength and temperature

The surface of snow changes in time, i.e. dry and porous fresh snow becomes wet and dense as the time elapses. Stronger reflection would return from wet and dense snow, and it causes stronger spectral peak of the multipath signature. Here, we examine if such a relationship exists. In Fig. 10, we plot the snow depth recovered by analyzing the SNR of the five satellites. These are the same data as in Fig. 8a, but with vertical offsets to discriminate data of different satellites. Here, we show the strength of the spectral peak (normalized by the largest strength of individual satellites) with color. Red and blue shows strong and weak peaks, respectively.

We can see that the reddish color prevails during the middle of March when daily maximum temperature exceeds 0°C and snow depth shows monotonous decrease due to thawing. On the other hand, peaks are weaker (bluish colors are dominant) after new snow falls, e.g. the first half of January. We can also see sporadic strong peaks around January 19, 23, and in the middle of February. These days are characterized by unseasonal warmness. On these days, maximum air temperatures exceeded 0°C and partial melting of the surface snow would have increased the reflectivity. These observations suggest the possibility of remotely sensing snow surface conditions by GPS.

5 Concluding remarks

We have shown that GPS and AMeDAS snow depth data agree with each other fairly well, i.e. GPS can measure snow depths accurate to ~10 cm as suggested earlier by Larson et al. (2009). We also found that L4 data could be used for the purpose, although SNR data give more precise results. Our results also suggest that even the lower quality L2P SNR data perform well in inferring snow depths. Then, the higher quality L2C SNR data would give even more accurate results. A systematic underestimation of ~10 cm common for L4 and SNR was found. At the moment, we cannot tell whether this is a real snow depth difference or an artifact due to microwave penetration into snow. Further studies are needed to solve this problem. We want to emphasize that we do not aim at the mm accuracy in GPS snow depth meter. A 10-cm error is equivalent to 20% of 50-cm deep snow. Although this is not a very accurate measurement, it would be useful for hydrologi-

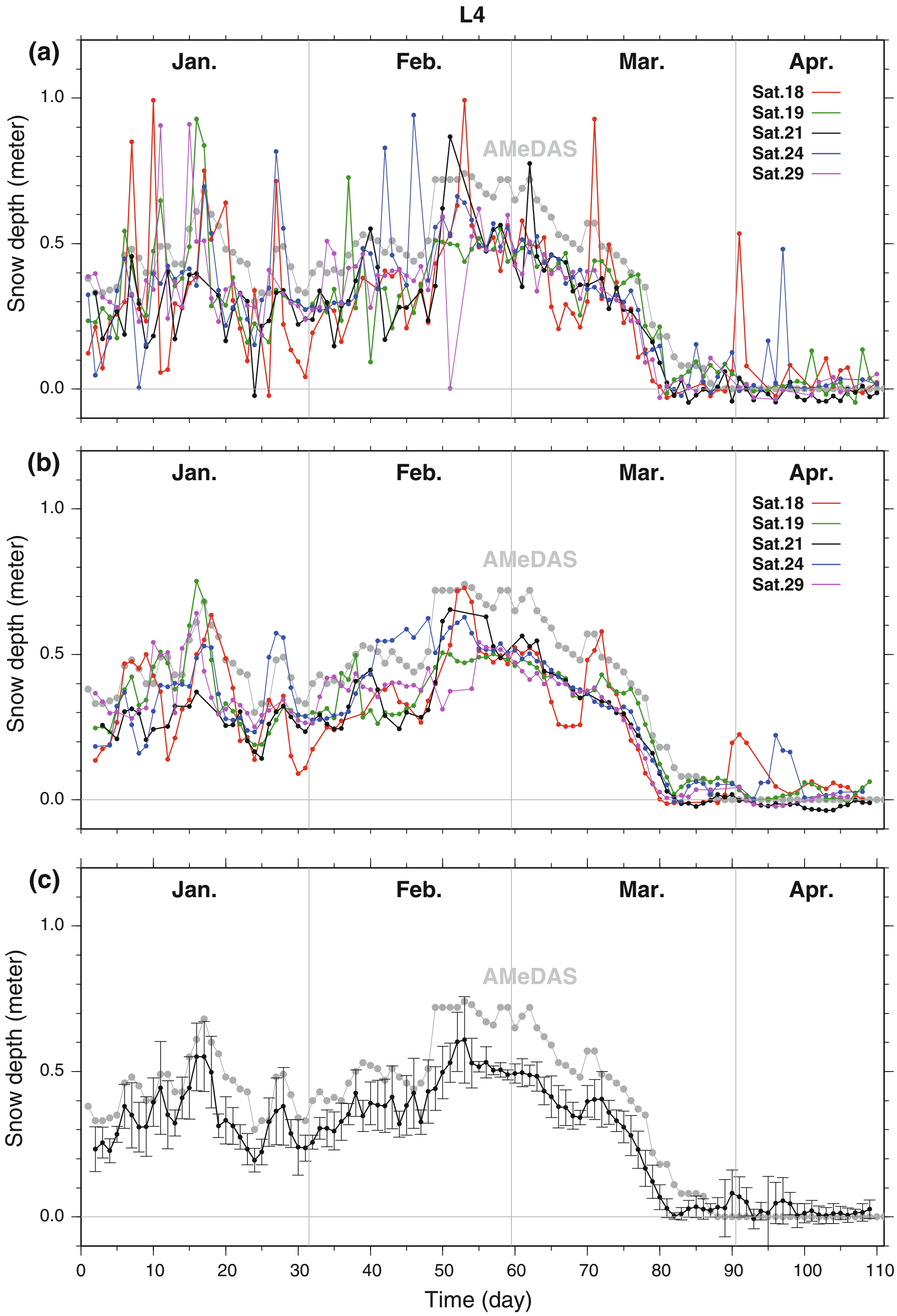

Fig. 7 **a** Raw snow depth time series obtained using L4 data from satellites 18, 19, 21, 24, and 29. The AMeDAS snow depth time series are shown with gray dots. **b** To reduce noise, spectrograms of the three consecutive days have been stacked to estimate the spectral peak of the middle day. **c** Daily averages of the snow depths by the five satellites in **b**. The *error bars* show one standard deviation, and the average standard deviation was ~0.062 m. The whole time series is shifted negatively from AMeDAS by ~0.1 m

cal and climatological communities (Larson et al. 2009). Because L4 is influenced by changes in ionosphere (observation in this paper was performed during the sunspot minimum), it should be examined if L4 works well under higher solar activities. It would be also meaningful to study if L4 can be used for other applications of GPS multipath, such as the measurements of soil moisture and vegetation growth.

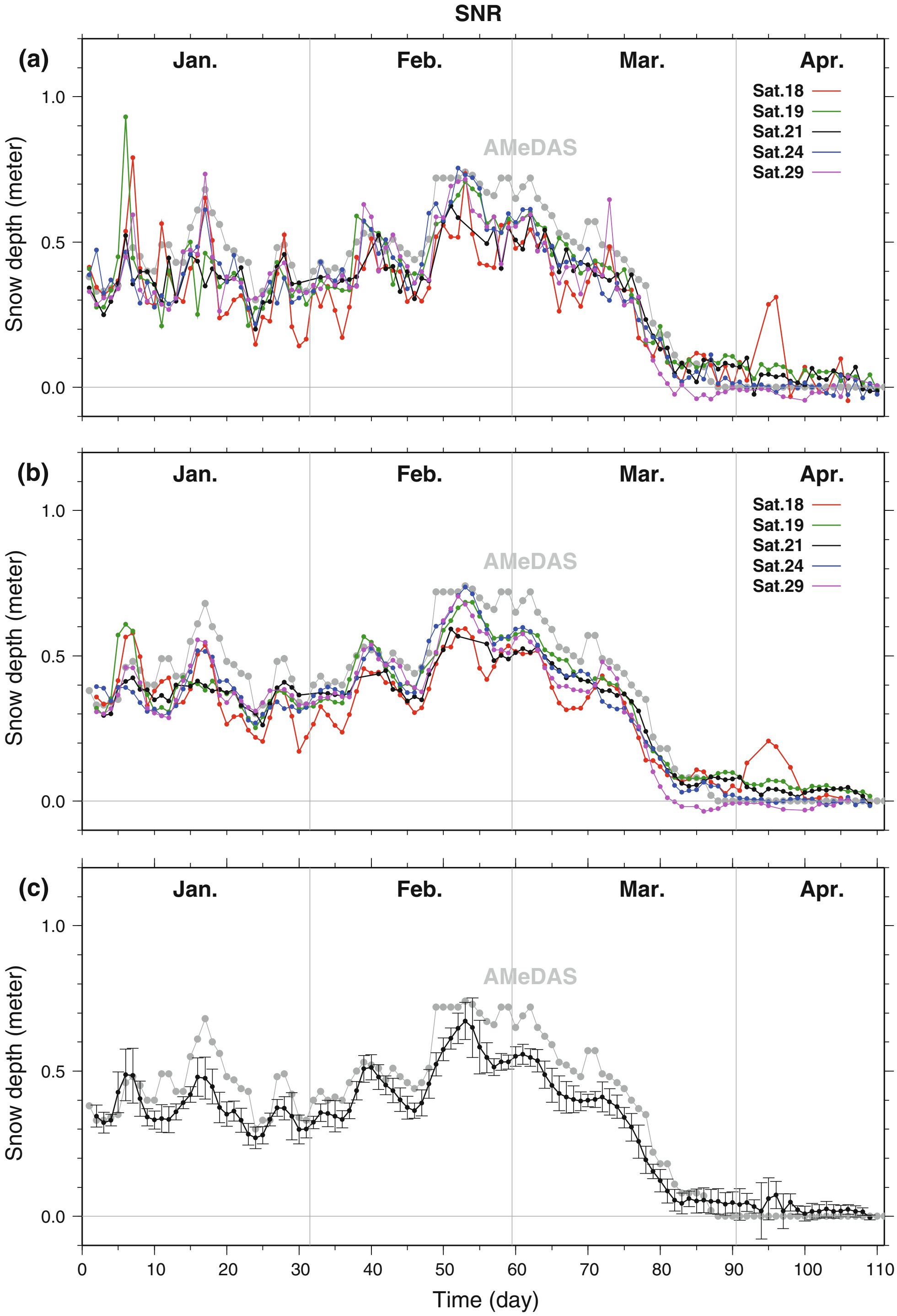

Fig. 8 Snow depth time series obtained using SNR data from satellites 18, 19, 21, 24, and 29. See the caption of Fig. 7 for detail. The average of the standard deviation was ∼0.041 m

L4 and SNR data are measured quite differently: the latter is derived from the intensities of the received microwave signals while the former is derived from their phases. Therefore, it is interesting that the snow depths from L4 and SNR data agree with each other. Although SNR data are more suitable to analyze multipath, it is important that L4 data could be used as a substitute. In 2009, GSI decided to add SNR data to the GEONET raw data files, recognizing that they are useful in analyzing multipath signatures. The files before 2009, however, still do not include them. Those from GPS networks worldwide do not always include SNR data. On the other hand, data files of any dual-frequency GPS stations

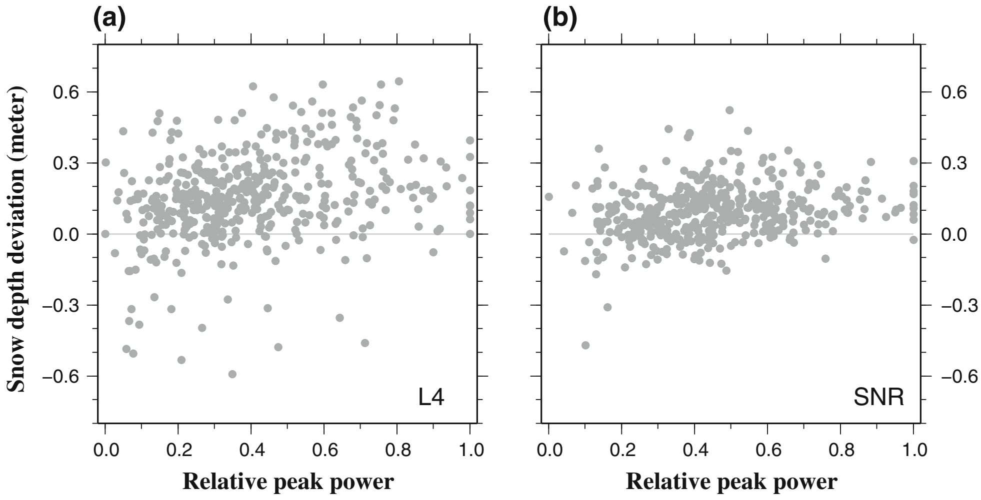

Fig. 9 Relationship between relative peak power strength and the deviation of the snow depths (AMeDAS minus GPS) by L4 (**a**) and SNR (**b**). Peak power is taken relative to the day of the largest power for individual satellites

Fig. 10 Snow depth estimated by analyzing the SNR data of the five satellites (whose *numbers* are attached to the *right*), with *colors of symbols* showing the relative strength of the peak. Individual time series are given vertical offset to facilitate visualization. At the *bottom*, we show daily average (*black curve*), maximum (*red*), and minimum (*blue*) temperature at the Shinshinotsu AMeDAS station

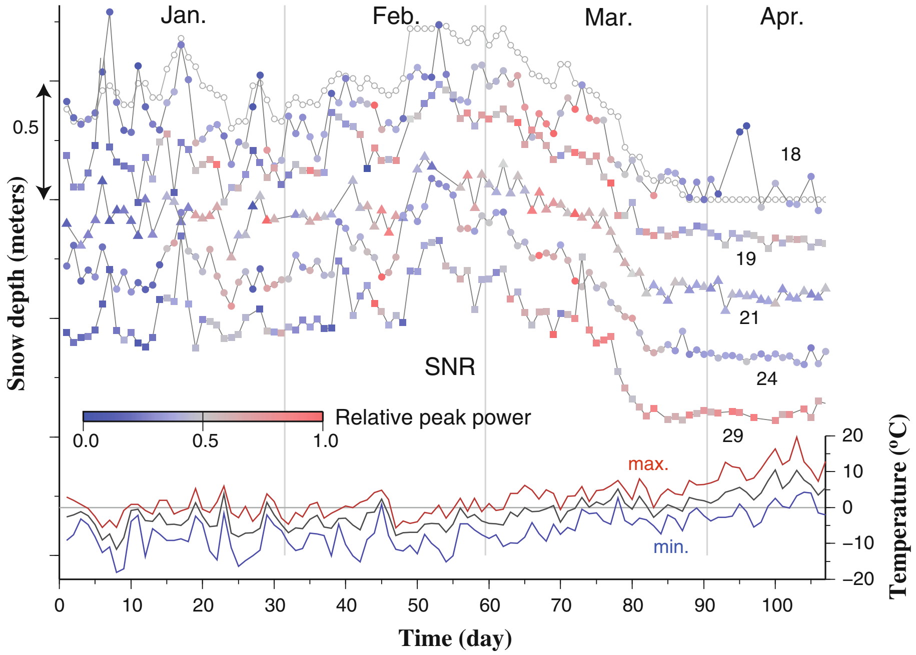

include L1 and L2 phases, and they could be used to analyze multipath with L4.

GPS snow depth meters measure the averages of snow depths over an extensive area (∼300 m^2 in the present case). To make a GPS station work as a snow depth meter, the ground should be clear of obstacles within ∼50 m from a 5 m high GPS antenna (Fig. 4b). This requirement becomes ∼20 m if the antenna height is 2 m. The open ground need not be in every direction. In the present case, ground to the south (SE-S-SW) was enough to observe five satellites. We should also avoid obstacles with heights such as trees beyond these reflecting grounds because they may block microwave signals before being reflected at the snow surface.

This open space requirement causes a problem in a densely populated country like Japan. For example, at the Shinshinotsu station studied here, a new two-story building (the Shinshinotsu Junior High School) was built to the south of the GPS antenna in summer 2009. Snow to the south of the antenna is now routinely removed. Hence, snow depth measurements there have been impossible since then (although positioning accuracy has not been much affected).

GPS could complement the AMeDAS network without introducing new infrastructure. There are ∼300 AMeDAS sensors which measure snow depths in Japan. On the other hand, there are >1,200 GPS antennas of GEONET stations throughout Japan. Using only a part of the stations fulfilling the space requirement as snow depth meters would bring a significant densification of the snow depth measurement network. In addition, we can measure snow depths by using GPS in countries where few or no snow depth sensors are available. It could contribute a great deal to global climatological and hydrological studies.

Acknowledgments We are grateful to Kristine Larson, University of Colorado, and two anonymous referees for constructive reviews. GEONET data were downloaded from ftp://terras.gsi.go.jp.

References

Bilich AL, Larson KM, Axelrad P (2008) Modeling GPS phase multipath with SNR: case study from the Salar de Uyuni, Bolivia. J Geophys Res 113:B04401. doi:10.1029/2007JB005194

Eloségui P, Davis JL, Jaldehag RK, Johansson JM, Niell AE, Shapiro B (1995) Geodesy using the global positioning system: the effects of signal scattering. J Geophys Res 100:9921–9934

Heki K, Ping JS (2005) Directivity and apparent velocity of the coseismic ionospheric disturbances observed with a dense GPS array. Earth Planet Sci Lett 236: 845–855. doi:10.1016/j.epsl.2005.06.010

Hino M (1984) Spectrum analysis. Asakura-Shoten, Tokyo, pp 300 (in Japanese)

Hofman-Wellenhof B, Lichtenegger H, Collins J (2001) GPS—theory and practice, 5th edn. Springer, New York, p. 382

Iizaka J (1998) Handbook of synthetic aperture radar images—new technique in Earth's environment measurement. Asakura-Shoten, Tokyo, p 208 (in Japanese)

Kedar S, Hajj GA, Wilson BD, Heflin MB (2003) The effect of the second order GPS ionospheric correction on receiver positions. Geophys Res Lett 30:1829. doi:10.1029/2003GL017639

Larson KM, Small EE, Gutmann ED, Bilich AL, Axelrad P, Braun JJ (2008) Using GPS multipath to measure soil moisture fluctuations: initial results. GPS Sol 12: 173–177. doi:10.1007/s10291-007-0076-6

Larson KM, Small EE, Gutmann ED, Bilich AL, Braun JJ, Zavorotny VU (2008) Use of GPS receivers as a soil moisture network for water cycle studies. Geophys Res Lett 35:L24405. doi:10.1029/2008GL036013

Larson KM, Gutmann ED, Zavorotny VU, Braun JJ, Williams MW, Nievinski FG (2009) Can we measure snow depth with GPS receivers?. Geophys Res Lett 36:L17502. doi:10.1029/2009GL039430

Larson KM, Braun JJ, Small EE, Zavorotny VU, Gutmann ED, Bilich AL (2010) GPS multipath and its relation to near-surface soil moisture content. IEEE J Sel Topics Appl Earth Obs Remote Sens 3(1). doi:10.1109/JSTARS.2009.2033612

Mannucci AJ, Wilson BD, Yuan DN, Ho CH, Lindqwister UJ, Runge TF (1998) A global mapping technique for GPS-derived ionospheric total electron content measurements. Radio Sci 33: 565–582. doi:10.1029/97RS02707

Ozeki M, Heki K (2010) Ionospheric holes made by ballistic missiles from North Korea detected with a Japanese dense GPS array. J Geophys Res 115:A09314. doi:10.1029/2010JA015531

Shoji Y, Kunii M, Saito K (2009) Assimilation of nationwide and global GPS PWV data on heavy rainfall in the 28 July 2008 Hokuriku and Kinki, Japan. SOLA 5:45–48

Small EE, Larson KM, Braun JJ (2010) Sensing vegetation growth with reflected GPS signals. Geophys Res Lett 37:L12401. doi:10.1029/2010GL042951

Zavorotny VU, Larson KM, Braun JJ, Small EE, Gutmann ED, Bilich AL (2010) A physical model for GPS multipath caused by land reflections: toward bare soil moisture retrievals. IEEE J Sel Topics Appl Earth Obs Remote Sens 3(1). doi:10.1109/JSTARS.2009.2033608